Evaluating ammonia (NH_3) predictions in the NOAA National Air Quality Forecast Capability (NAQFC) using *in-situ* aircraft and satellite measurements from the CalNex2010 campaign

Casey D. Bray,[1*] William Battye,[1] Viney P. Aneja,[1]
Daniel Tong,[2,3,4] Pius Lee[2] , Youhua Tang[2,3]
and John B. Nowak[5]

***Corresponding author:**
Email: cdbray@ncsu.edu
Telephone: (919) 515-7808

To be submitted: Atmospheric Environment
May 2017

[1] North Carolina State University, Raleigh, NC 27695
[2] NOAA Air Resources Laboratory, 5830 University Research Court, College Park, Maryland, MD 20740
[3] Cooperative Institute for Climate and Satellites, University of Maryland, College Park, Maryland, MD 20740
[4] Center for Spatial Information Science and Systems, George Mason University, Fairfax, Virginia, VA 22030
[5] Aerodyne Research, Inc. Billerica, MA 01821

Abstract:

Atmospheric ammonia (NH_3) is not only a major precursor gas for fine particulate matter ($PM_{2.5}$), but it also negatively impacts the environment through eutrophication and acidification. As the need for agriculture, the largest contributing source of NH_3, increases, NH_3 emissions will also increase. Therefore, it is crucial to accurately predict ammonia concentrations. The objective of this study is to determine how well the U.S. National Oceanic and Atmospheric Administration (NOAA) National Air Quality Forecast Capability (NAQFC) system predicts ammonia concentrations using their Community Multiscale Air Quality (CMAQ) model (v4.6). Model predictions of atmospheric ammonia are compared against measurements taken during the NOAA California Nexus (CalNex) field campaign that took place between May and July of 2010. Additionally, the model predictions were also compared against ammonia measurements obtained from the Tropospheric Emission Spectrometer (TES) on the Aura satellite. The results of this study showed that the CMAQ model tended to under predict concentrations of NH_3. When comparing the CMAQ model with the CalNex measurements, the model under predicted NH_3 by a factor of 2.4 (NMB = -58%). However, the ratio of the median measured NH_3 concentration to the median of the modeled NH_3 concentration was 0.8. When compared with the TES measurements, the model under predicted concentrations of NH_3 by a factor of 4.5 (NMB = -77%), with a ratio of the median retrieved NH_3 concentration to the median of the modeled NH_3 concentration of 3.1. Because the model was the least accurate over agricultural regions, it is likely that the major source of error lies within the agricultural emissions in the National Emissions Inventory. In addition to this, the lack of the use of bidirectional exchange of NH_3 in the model could also contribute to the observed bias.

1. Introduction and Background

Ammonia (NH_3) is an important gas in the atmosphere. Major sources of NH_3 include livestock, fertilizer, soil, biomass burning, industry, vehicles, the ocean, humans, and waste disposal/recycling activities, with agricultural emissions accounting for about 90% of NH_3 emissions into the atmosphere (Anderson *et al.,* 2003; Aneja *et al.,* 2009). As the world's population continues to increase, the fertilizer and agricultural (both crop and animal) industries will also increase, thus leading to increasing NH_3 emissions into the atmosphere (Heald *et al.,* 2012), which could cause a number of impacts to both human health and the environment.

NH_3 reacts with sulfuric, nitric and hydrochloric acids to form ammonium sulfate, ammonium bisulfate, ammonium nitrate and ammonium chloride aerosols, all of which contribute to the formation of fine particulate matter ($PM_{2.5}$) (Robarge *et al.*, 2002; Baek and Aneja, 2004; Baek *et al.,* 2004; Renner and Wolke, 2010; Wang *et al.*, 2012; Kwok *et al.*, 2013). Exposure to elevated $PM_{2.5}$ concentrations is a major concern for human health and welfare due to the particles' ability to penetrate deep into the respiratory tract. There are many adverse health effects associated with elevated concentrations of fine particulate matter, such as cardiovascular and respiratory issues and even death (Anderson *et al.,* 2003; Pope *et al.*, 2009; Behera and Sharma, 2010a, b). Fine particulate matter is also associated with a number of environmental impacts, such as reducing visibility and changing the earth's radiational balance (Behera and Sharma, 2010a, b; Fan *et al.,* 2005; Heald *et al.,* 2012; Wang *et al.*, 2012).

In addition, NH_3 is also important in the environment due to its role in acid deposition and the nitrogen cycle, which is one of the most important nutrient cycles for living organisms. NH_3 and ammonium (NH_4^+) in the atmosphere are deposited to the surface via wet and dry deposition, thus increasing the amount of reduced nitrogen (Robarge *et al.,* 2002). This could lead to a number of negative impacts on the environment, such as soil acidification, eutrophication, as well as decreasing the resistance of vegetation to drought and frost damage (Robarge *et al.,* 2002). NH_3 in agricultural soil also plays a significant role in the formation of nitrous oxide (N_2O), a major greenhouse gas. The oxidation of NH_3 during the nitrification process can produce N_2O in a number of different pathways, such as through the denitrification process.

Due to the importance of atmospheric NH_3, it is necessary that the air quality models are able to accurately predict concentrations of NH_3. The purpose of this research is to determine how accurate the National Oceanic and Atmospheric Administration's (NOAA) National Air Quality Forecast Capability (NAQFC), which uses the Community Multiscale Air Quality (CMAQ) model (v4.6), predicts NH_3 and ammonium concentrations during the CalNex2010 (California Nexus) field campaign. During the CalNex2010 field campaign, *in-situ* measurements of pollutants were obtained via aircraft between May and July, 2010, across much of California (Ryerson *et al.,* 2013). Figure 1 shows the flight paths taken during the field campaign.

Model predictions of NH_3 and NH_4^+ are compared with measurements taken via aircraft as well as with satellite measurements obtained from the Tropospheric Emission Spectrometer (TES) aboard NASA's Aura satellite in order to determine the accuracy of NOAA's CMAQ model. Because agricultural emissions of NH_3 are difficult to quantify, there is much uncertainty in the emission inventory used by the CMAQ model. The objective of this research is to not only determine the accuracy of NOAA's CMAQ model, but also to

identify potential ways to improve the NH_3 emissions inventory used in the CMAQ model for California.

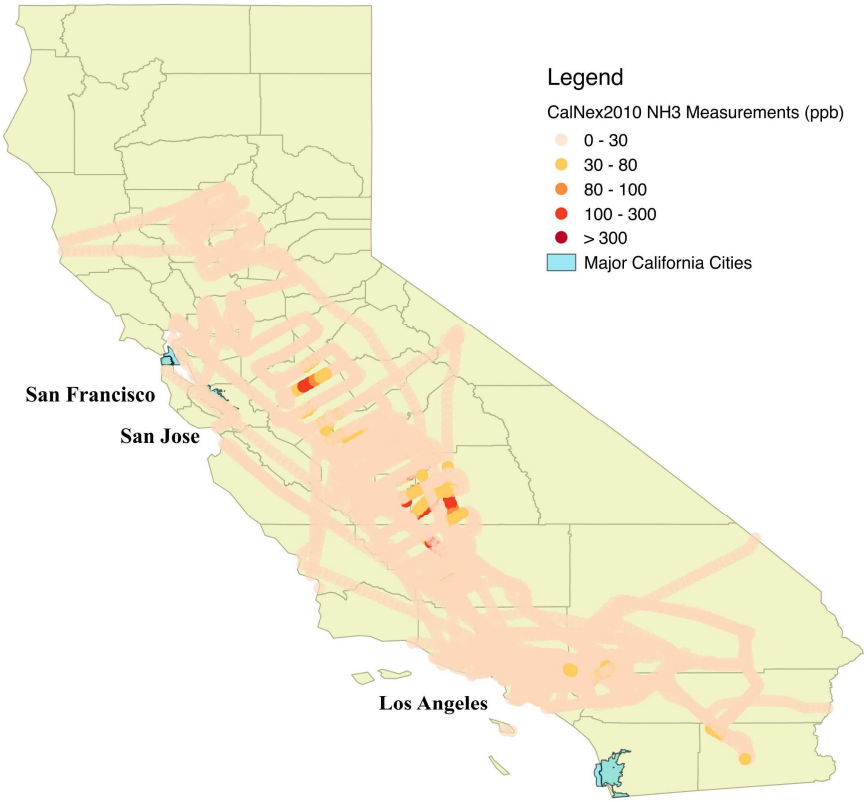

Figure 1. The flight paths taken during the CalNex field campaign, with the colored dots representing locations where NH_3 measurements were made. The blue polygons represent major California cities for reference.

2. Methodology

2.1. Air Quality Model

Version 4.6 of the CMAQ model, using the CB05-AERO5 chemical mechanism, was used to predict the concentrations of NH_3 and NH_4^+, at 12 km grid resolution, from May to July, 2010. The meteorological predictions used within the CMAQ model were generated by the North American Mesoscale Forecast System (NAM). The NH_3 and ammonium emissions used in the model were obtained via the 2005 US Environmental Protection Agency's (EPA) National Emissions Inventory (NEI). The emission data used in NOAA's NAQFC system was based on the 2005 US Environmental Protection Agency's (EPA) 2005 National Emissions Inventory (NEI), with an update using the Cross-State Air Pollution Rule (Pan *et al.,* 2015; Tong *et al.,* 2015; Canty *et al.*, 2015; Duncan *et al.,* 2015).

2.2. Aircraft Measurements

Daytime measurements of atmospheric NH_3 and NH_4^+ from NOAA's WP-3D aircraft from May 4th to June 20th, 2010, taken over California are used here. Gaseous NH_3 was

measured using chemical ionization mass spectrometry (CIMS) at 1 Hz (~100 m spatial resolution) with typical inaccuracies ± 30% ± 0.2 ppbv and a 1 σ uncertainties of 0.08 ppbv (Nowak *et al.*, 2010; Nowak *et al.*, 2012). NH_4^+ concentrations were measured using a compact time-of-flight mass spectrometer with 2σ uncertainties of ± 34% ± 0.06 μg m^{-3} (Bahreini *et al.,* 2009; Bahreini *et al.,* 2012; Nowak *et al.*, 2012). NH_4^+ was measured every 10 seconds and then averaged over one minute, while NH_3 was measured every second and then averaged over 1 minute (Nowak *et al.*, 2010; Nowak *et al.*, 2012). The one minute averages were compared with the model estimates. Measurements of NH_4^+ were taken in μg standard m^{-3}, where standard signifies that these measurements were taken at standard temperature and pressure, while measurements of NH_3 were taken in μg m^{-3}. Therefore, for this comparison, it was necessary to convert the μg standard m^{-3} to μg m^{-3} using measurements of the ambient atmosphere that were taken during the flight. Meteorological parameters including temperature, dew point temperature, potential temperature, relative humidity, wind speed and wind direction were measured (Ryerson *et al.*, 2013). In addition to this, the aircraft's navigation system and global positioning system (GPS) measured the location, altitude, speed, bearing and the angle of descent were recorded. The CMAQ model predictions of NH_3 and NH_4^+ (in μg m^{-3}) were used for comparison against each 1-minute aircraft measurement. The CMAQ prediction for each measurement location and time was computed by 4-dimensional interpolation across space and time, using the model grid centroids surrounding the measurement point for the hours before and after the measurement.

2.3. Satellite Measurements

Predictions from the CMAQ model were also compared against satellite NH_3 concentrations retrieved from infrared spectra gathered by the Tropospheric Emission Spectrometer (TES) on the National Aeronautics and Space Administration's (NASA) Aura satellite. TES is a high spectral resolution infrared Fourier Transform spectrometer (FTS) (Beer, 2006) that covers the spectral range 650–3050 cm (Bowman *et al.,* 2006). TES has a spatial resolution of 5.3 x 8.5 km nadir and 37 x 23 km limb and has a spectral resolution of 0.5 x 5 km nadir and 2.3 x 23 km limb (Beer *et al.,* 2001; Zhu *et al.,* 2013). TES measures the Earth's infrared light energy and follows a sun-synchronous orbit, making observations on a 16-day cycle, with roughly 1 pass during the day and 1 pass during the night over each region every other day (Clarisse *et al.,* 2010; Zhu *et al.,* 2013). Atmospheric ammonia concentrations are derived from TES by observing changes in the infrared radiation intensity between 940 cm^{-1} and 970 cm^{-1}. The TES ammonia retrievals use a forward radiative transfer model (RTM) to compute the expected intensity of radiation at the top of the atmosphere for an estimated ammonia concentration. The assumed concentration of ammonia is varied to minimize the error between the spectrum predicted by the RTM and the spectrum actually measured by the satellite. This results in an estimate of the vertical profile of the ammonia concentration for the region sensed by the satellite. (Bowman *et al.,* 2006; Shephard *et al.,* 2011; Shephard and Cady-Pereira, 2015). Finally, the meteorological conditions (temperature, relative humidity, etc.) are used with the a priori NH_3 profile to estimate the atmospheric NH_3 concentration (Herman and Osterman, 2014).

TES performed 6 transect measurements over the CalNex study domain between May 7, 2010, and June 3, 2010. In order to compare with the CMAQ model predictions, the NH_3

concentration for the aircraft sampling height was extracted from the total column data based on the assumed a priori profile. This study used only measurements that met TES Species Retrieval Quality criteria and for which the degrees of freedom for signal (DOFS) exceeded 0.5. It is important to note that there are some uncertainties associated with this data. For example, the satellite retrieval of ammonia concentration may be biased toward the a priori assumption. In addition to this, the estimated vertical distribution of ammonia is also impacted by the a priori assumption made.

.

2.4. Model to Measurement Comparisons

Similar to the work of Battye *et al.* (2016), the normalized mean bias (NMB) was calculated using the following equation:

$$NMB = \frac{1}{N}\frac{\sum_{i=1}^{N}[C_{mod}(i)-C_{obs}(i)]}{\sum_{i=1}^{N}C_{obs}(i)},$$

in order to determine the accuracy of the NAQFC CMAQ model. The ratio of the average measured concentration to the average model prediction ($R_{o/m}$) was calculated using:

$$R_{o/m} = \frac{\sum_{i=1}^{N}C_{obs}}{\sum_{i=1}^{N}C_{mod}},$$

where $C_{mod}(i)$ is the model prediction, $C_{obs}(i)$ is the observed concentration at a given location and time, and N is the number of observations. The relationship between NMB and $R_{o/m}$ is as follows:

$$NMB = \frac{1}{R_{o/m}} - 1.$$

3. Results and Discussion

3.1. Aircraft Measurements Compared with Model Predictions

Table 1 compares the aircraft measurements of NH_3 and NH_4^+ taken during the field campaign with the model predictions predicted by NOAA's CMAQ model and the calculated NH_x (NH_3 (g) + NH_4^+ (p)) concentrations. The average concentration of the 1-minute averaged NH_3 observations in the CalNex field campaign was 4.1 ± 14.8 ppbv (2.7 ± 9.9 µg m^{-3}), with a maximum 1-minute average concentration of 380.1 ppbv (254.7 µg m^{-3}) and a maximum 1-second concentration of 963 ppbv (669 µg m^{-3}). In contrast to this, the model predicted an average NH_3 concentration of 1.7 ± 2.4 ppbv (1.1 ± 1.4 µg m^{-3}), with the maximum predicted NH_3 concentration at 17.3 ppbv (11.3 µg m^{-3}). Thus, the measured concentration of NH_3 was a factor of 2.4 higher than what was modeled by the CMAQ forecasting model, with a normalized mean bias of -58%.

228 **Table 1.** Comparison of in situ aircraft measurements with model predictions for NH_3, NH_4^+, and NH_X.

	NH_3 (ppbv)	NH_3 ($\mu g\ m^{-3}$)	NH_4^+ ($\mu g\ m^{-3}$)	NH_X ($\mu g\ m^3$)
Measured concentrations				
Average	4.1	2.7	0.4	3.1*
Standard deviation	14.8	9.9	0.7	10.6*
Maximum	380.1	254.7	6.7	254*
Median	0.8	0.5	0.2	1.0
Model predictions				
Average	1.7	1.1	0.6	1.7*
Standard deviation	2.4	1.4	0.8	2.2*
Maximum	17.3	11.3	7.3	11.5*
Median	0.9	0.6	0.3	1.2*
Comparison statistics				
Normalized mean bias	-58%		43%	-44%
Ratio of average measured value to average modeled value	2.4		0.7	1.8
Ratio of median measured value to median modeled value	0.8		0.7	0.8
Correlation coefficient (r)	0.34		0.62	0.30
Coefficient of determination (r^2)	0.12		0.38	0.09
Number of observations	8,181		4,605	4,605

229 * Denotes calculated value, not measured

230

231 In order to take out the influence of the outlier data points, the median was also calculated
232 for the modeled and measured NH_3 concentration. The median NH_3 concentration measured
233 in the field campaign was 0.8 ppbv (0.5 $\mu g\ m^{-3}$), while the median modeled concentration
234 was 0.9 ppbv (0.6 $\mu g\ m^{-3}$). The ratio of the measured median concentration and the modeled
235 median concentration of ammonia is 0.8, which suggests that the model is fairly accurate
236 without the influence of the elevated outlier NH_3 concentrations observed in the field
237 campaign.
238 Figure 2 shows the measured concentrations of NH_3 (y-axis) compared with the model
239 predictions of NH_3 (x-axis) on a log-log scale plot, with the plotted measurements
240 represented as the blue dots, the gold line representing the actual measured trend line, the
241 cyan-green line representing the bias line given by the ratio of the medians and the red line
242 representing where the measured points would have fallen if the model correctly predicted
243 the measurements. The log-log plot was chosen for this figure due to the large range
244 observed in measured ammonia concentrations. When comparing the actual trend line with
245 the modeled one-to-one line (i.e. when the measured = modeled), it appears that the model
246 under predicted concentrations of NH_3 by a factor of 2.4. However, when comparing the
247 one-to-one line with the bias line given by the median ratio, it appears that the model only
248 under predicted NH_3 concentrations by a factor of 0.8.

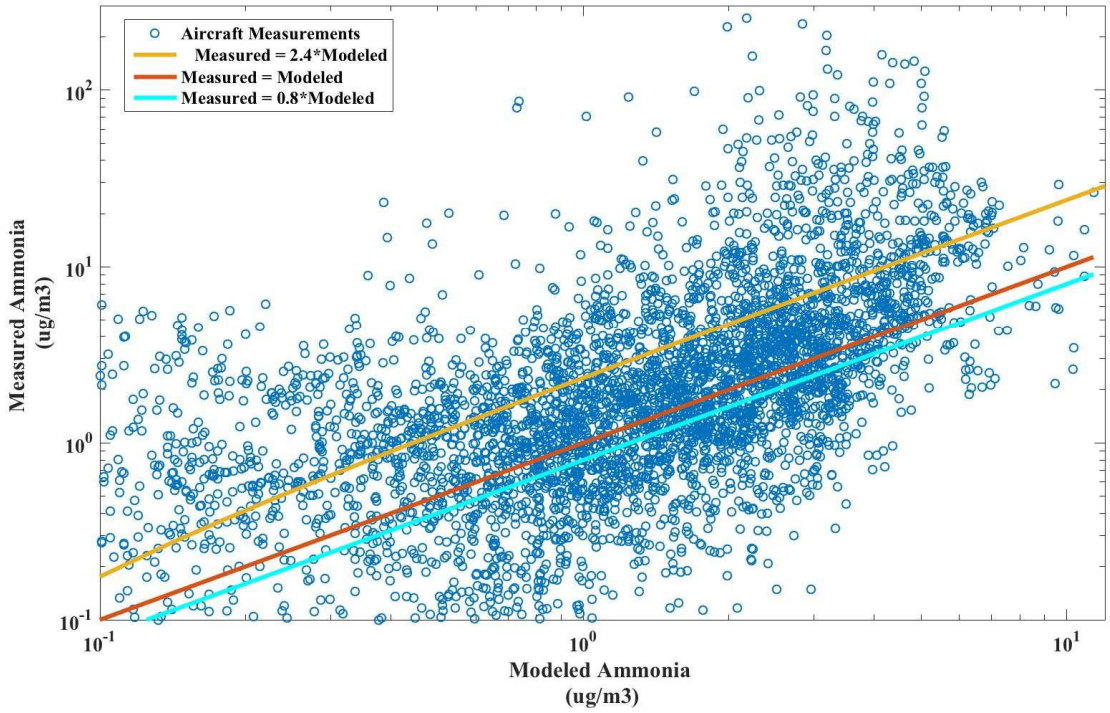

Figure 2. Aircraft *in-situ* measurements of NH_3 (blue dots) plotted against model predictions on a log-log scale plot. The red line shows where the measured points should have fallen if the model predictions were exactly correct and the gold line shows the actual measured trend line. The actual trend line (gold line) is plotted above the one-to-one line (red line), while the bias line given by the median ratio is given by the cyan-green line.

The average NH_4^+ concentration for the CalNex study area was found to be 0.4 ± 0.7 µg/m^3, with a maximum concentration of 6.7 µg m^{-3}. In comparison, the CMAQ model predicted an average NH_4^+ concentration of 0.6 ± 0.8 µg m^{-3}, with a maximum predicted concentration of 7.3 µg m^{-3}. The concentration of NH_4^+ for the study area was found to be a factor of 0.7 lower than the prediction made by the CMAQ model and the calculated normalized mean bias was found to be 43%. When comparing the median values of the measured and modeled data, the measured NH_4^+ median was 0.2 µg m^{-3} and the modeled NH_4^+ median was 0.3 µg m^{-3}. This corresponds to a ratio of the measured to modeled median concentration of 0.7, which is equivalent to the ratio of the modeled to measured concentration. Figure 3 shows the comparison of the measured concentration of NH_4^+ compared with the modeled concentrations, plotted with the observed trend line (gold) and the one-to-one line (red). It is necessary to note that the bias line given by the median ratio is not shown because it is equivalent to the observed trend line. Because both the modeled and measured ammonium concentrations were less than 10 µg m^{-3}, this figure was plotted on a linear scale as oppose to a log-log scale. Unlike the comparison with NH_3 concentrations, the modeled NH_4^+ concentrations were fairly close to the measurements made, with the model slightly over predicting, particularly at higher concentrations of NH_4^+. This suggests that the model had a fairly good handle on the conversion of gaseous NH_3 to particulate ammonium and thus the conversion was likely not limited by the concentration of gaseous NH_3.

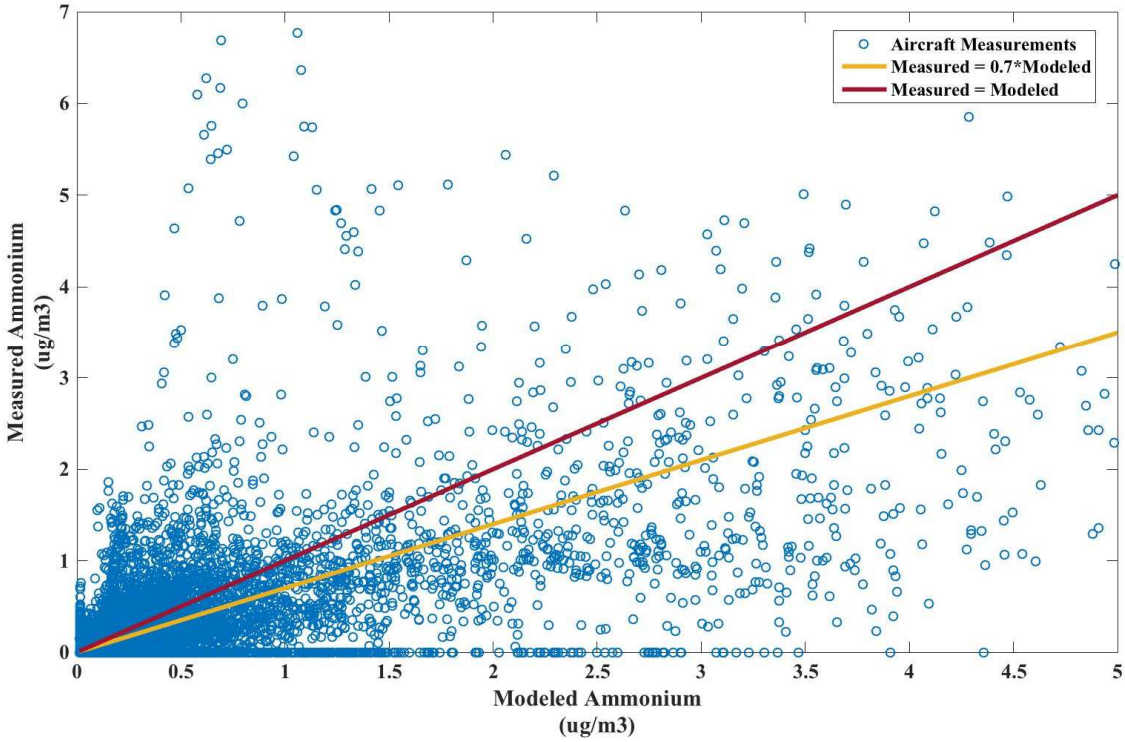

Figure 3. Aircraft *in-situ* measurements of NH_4^+ (blue dots) plotted against model predictions on a linear scale plot. The red line shows where the measured points should have fallen if the model predictions were exactly correct, the gold line shows the actual measured trend line. In this case, the bias line is equivalent to the actual trend line and is therefore not plotted in Figure 3.

The average concentration of NH_x measured during the field campaign was 3.1 ± 10.6 µg m^{-3}, with a maximum concentration of 254 µg m^{-3}. In comparison to this, the CMAQ model predicted an average concentration of 1.7 ± 2.2 µg m^{-3}. The maximum predicted NH_x concentration was 11.5 µg m^{-3}. The measured concentration of NH_x was found to be a factor of 1.9 higher at very low concentrations ($<10^{-0.5}$) of NH_x than what was predicted by the CMAQ model and a factor of 1.9 lower than what was predicted by the CMAQ model at higher concentrations. The average measured to modeled ratio of 1.9 corresponds to a normalized mean bias of -44%. However, comparing the medians of the measured and modeled NH_x concentration, the medians were found to be 1 µg m^{-3} and 1.2 µg m^{-3}, respectively. This corresponds to a median ratio of 0.8, which is lower than the ratio that was observed when comparing the average modeled NH_x concentrations with the average measured NH_x concentrations. Figure 4 shows the comparison of the measured concentration of NH_4^+ compared with the modeled concentrations on a log-log scale plot. Similar to Figure 2, this was also plotted on a log-log due to the large range in measured NHx concentrations. As described above, this figure shows the model tends to under predict concentrations of NH_x at higher concentrations of NH_x and the model tends to over predict concentrations of NH_x at lower concentrations. However, when comparing the bias line of the median ratio (cyan-green line) with the one-to-one line (red line) it appears that the measured values are fairly close to the modeled projections.

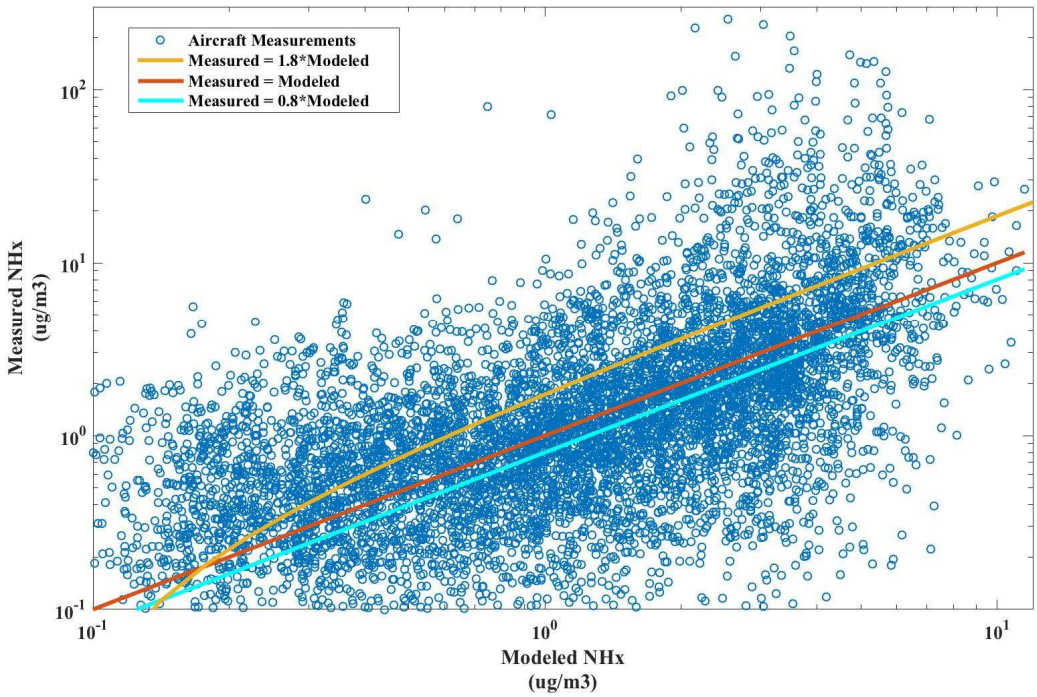

Figure 4. Calculations based off of aircraft *in-situ* measurements (referred to as measured), of NH_x (blue dots) plotted against calculated model predictions (referred to as modeled) on a log-log scale plot. The red line shows where the measured points should have fallen if the model predictions were exactly correct, the yellow line shows the actual measured trend line, and the cyan-green line shows the bias line given by the median ratio.

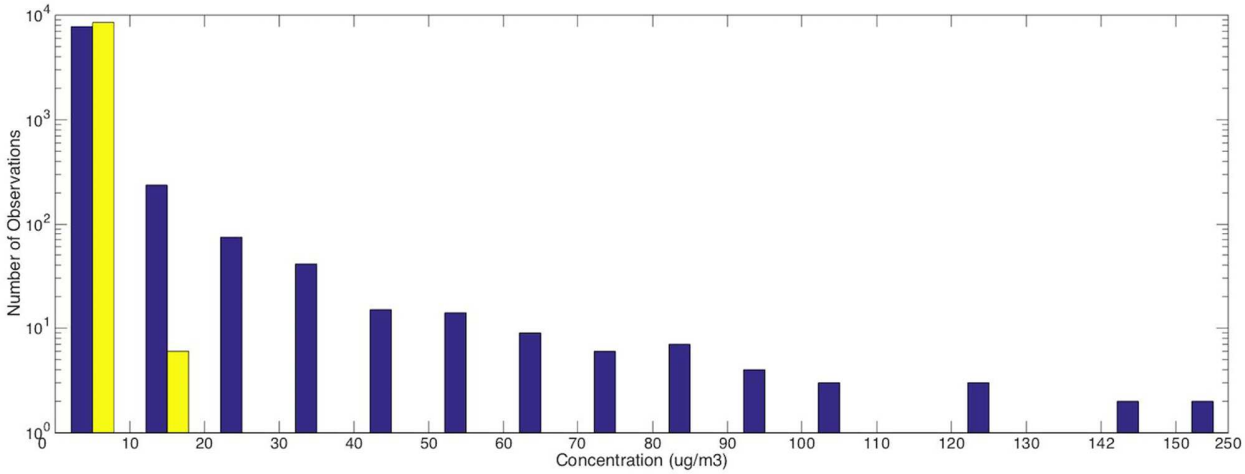

Figure 5. Histogram comparing the modeled (yellow) versus the measured (purple-blue) NH_3 concentration with respect to the number of observations. Both the modeled and the measured concentration of NH_3 occurred most frequently at lower concentrations. However, the range of observations at different concentrations is much larger for measured values. This suggests that there was a greater variation in the concentration measured as oppose to the modeled concentration, which occurred primarily at concentrations less than 30 µg m^{-3}.

Figure 5 shows a histogram comparing the modeled and measured NH_3 concentrations. The extreme values measured during the field campaign are significantly higher than the

extreme values predicted by the model. While both the modeled and measured concentrations show a similar negative pattern, where the number of observations is highest at the lowest concentration and then rapidly decreases thereafter, the slope of the decrease is significantly different. The number of observations from the field campaign gradually decreases with increasing ammonia concentrations while the number of modeled observations drop exponentially with increasing ammonia concentrations, such that there are no observations above 30 $\mu g\ m^{-3}$. The 98th percentile of the measured NH_3 values was found to be 23.2 $\mu g\ m^{-3}$ while the 98th percentile of the modeled NH_3 values was 5.1 $\mu g\ m^{-3}$, showing the vast under estimation of NH_3 concentrations by the model.

Spatial patterns in the model prediction error were identified by comparing the model bias (model concentration – measured concentration) in relation to NH_3 point sources and agricultural sources. Figure 6 plots both the agricultural and point source emissions (obtained from the US EPA's National Emissions Inventory) with relation to the model bias. Figure 6A shows all the calculated model bias for the period while Figure 6B only shows model bias over 50 ppbv.

The majority of the high model biases occur over large agricultural regions and the highest model bias occurs over point sources. This suggests that the 2005 NEI under predicts NH_3 concentrations within this region of California. When comparing the 2005 NEI NH_3 emissions with the 2011 NH_3 NEI emissions for the study domain, it is found that there is a 25% increase in the NH_3 emissions, which would certainly account for some of the observed bias. However, the 2014 NEI NH_3 emissions, which uses an entirely different methodology for their agricultural emissions, are 62% higher than the 2011 NEI NH_3 emissions and 85% higher than the 2005 NEI NH_3 emissions (EPA, 2005; EPA, 2011; EPA, 2014). According to the US EPA 2014 National Emissions Inventory (version 1) Technical Supporting Document, this version of the NEI has updated the agricultural livestock ammonia methodology in order to incorporate both new observational data as well as new process based methods. In addition to this, the methodologies used to develop emissions from fertilizer application have been entirely changed. For example, in this inventory, ammonia emissions from agricultural soils are estimated using the bidirectional version of the CMAQ model (v5.0.2) coupled with the Fertilizer Emissions Scenario Tool for CMAQ FEST-C(v1.2) (EPA, 2016). Based on this, it is likely that the agricultural emissions used in the model contributed to much of the biases observed in this study.

Another potential cause for the discrepancies between the model and the measured values could be the NEI's handle on the diurnal and seasonal representation of ammonia emissions in this region. However, it is important to note that the diurnal represntation of ammonia emissions has been updated within the Sparse Matrix Operator Kernel Emissions (SMOKE) model and this has been released in the newer (2011, 2014) versions of the NEI (Zhu et al., 2015).

3.2. Model Predictions Compared with Satellite Retrievals

The CMAQ model prediction of NH_3 was compared with the TES satellite retrieval of concentrations measured at the CalNex aircraft measurement heights (Table 2, Figure 7a). The average TES NH_3 concentration was 14.8 ± 11.8 $\mu g\ m^{-3}$, with a maximum retrieved concentration of 40.5 $\mu g\ m^{-3}$ and a median concentration of 10.4 $\mu g\ m^{-3}$, while the associated average CMAQ model concentration was found to be 3.3 ± 1.0 $\mu g\ m^{-3}$, with a maximum predicted concentration of 4.9 $\mu g\ m^{-3}$ and a median concentration of 3.4 $\mu g\ m^{-3}$.

As Figure 7a shows, the majority of the NH_3 retrieval measurements fall above the one to one line (where the modeled NH_3 = the TES NH_3 retrieval), which suggests that the TES retrieval measurements are higher than the concentrations predicted by the model. This normalized mean bias of the TES retrieval was found to be -77%, which corresponds to a ratio of the average measured NH_3 value to the average NH_3 TES retrieval of 4.5. Similarly, the ratio of the median measured value to median modeled value was 3.1. The average total column loading (mg m^{-2}) measured by TES was 7.2 ± 6.7 mg m^{-2}, with a maximum total column loading of 40 mg m^{-2} and a median value of 5.1 mg m^{-2}. In contrast to this, the average total column loading predicted by the CMAQ model was 0.002 ± 0.002 mg m^{-2}, with a maximum total column loading of 0.008 mg m^{-2} and a median of 0.002 mg m^{-2} (Table 2, Figure 7b). This corresponds with a NMB of -99% and a ratio of the average measured NH_3 value to the average NH_3 TES retrieval 3600. The ratio of the median measured value to median modeled value was 2550. Because the satellite samples a larger volume of air than the CIMS, it is expected that the retrieved range of concentrations of ammonia would be narrower than those observed by the aircraft due to the fact that there is much more variability on a smaller spatial scale. In addition to this, it would follow that the satellite retrievals would also be lower than those observed by the aircraft (assuming the aircraft was targeting emission sources), due to the fact that the concentration of atmospheric ammonia drops exponentially with increasing distance from the source, thus returning values that are similar to the volume modeled by CMAQ. While the authors tried to pair the CMAQ/aircraft measurement data with the TES retrievals such that they were as close as possible, a potential reason for the discrepancies between the TES NH_3 retrieval and the CMAQ model estimates, could be due to the fact that the measurements did not align 100% in time and space.

A

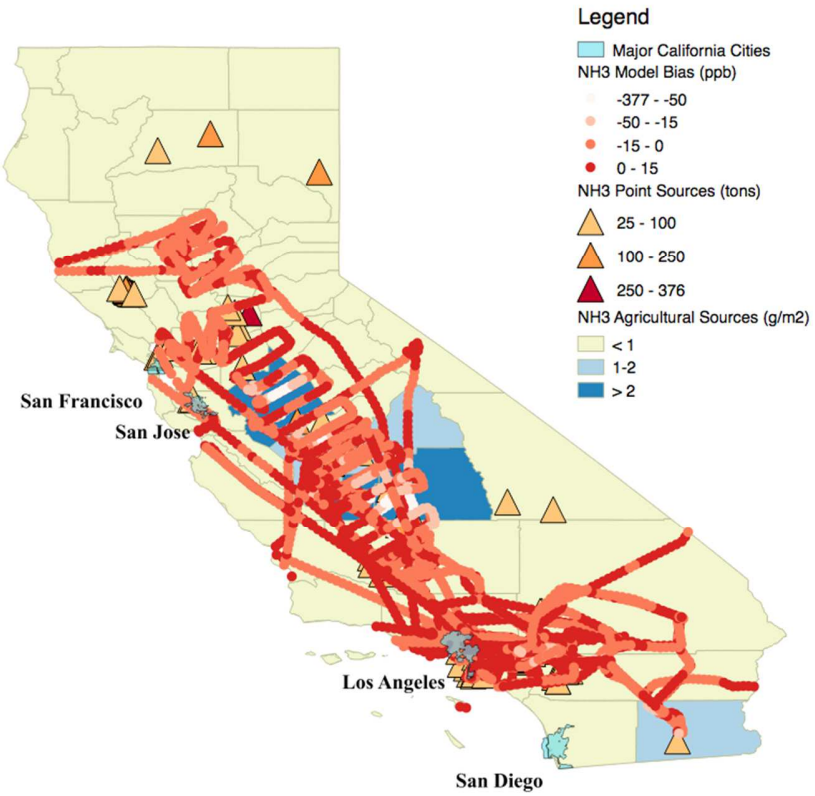

B

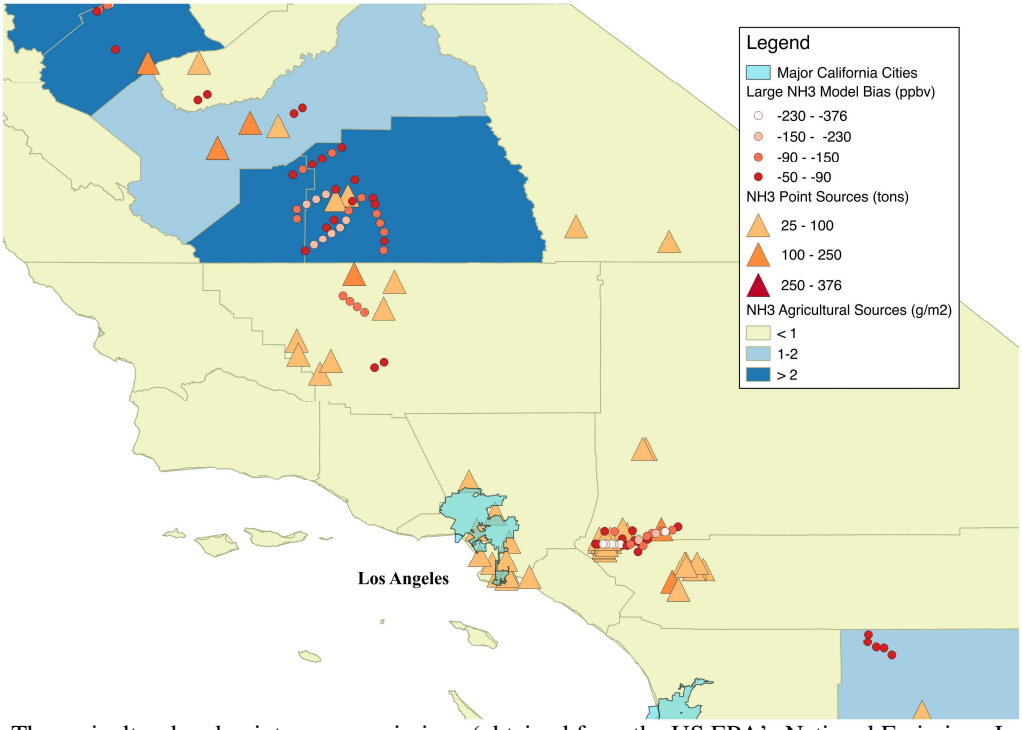

Figure 6. The agricultural and point source emissions (obtained from the US EPA's National Emissions Inventory) plotted with relation to the model bias. Figure 6A shows all the model biases obtained from the CalNex study while Figure 6B shows only the largest model bias. Note that major under estimates occurred in close proximity to both NH_3 point sources as well as agricultural sources of NH_3.

A.

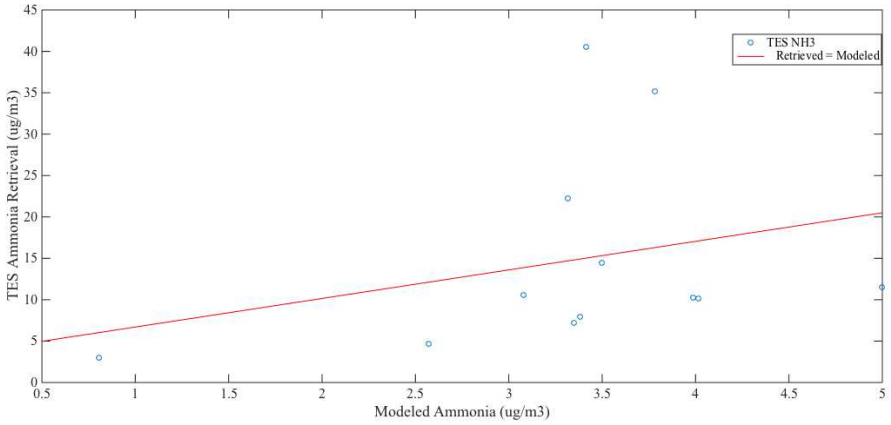

B.

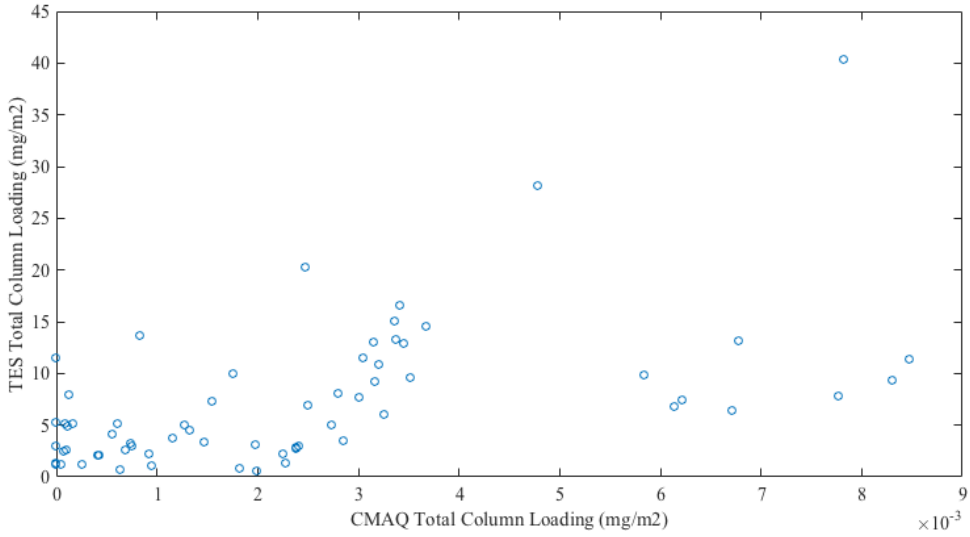

Figure 7. The CMAQ model prediction of NH_3 compared with the TES satellite retrieval at the aircraft measurement level plotted on a log-log scale plot (A) and the model the total column loading compared with the TES total column loading retrieval (B). The red line in Figure 7A shows where the TES retrieval points should have fallen if the model predictions were exactly correct. Looking at the order of magnitude, it is evident that the modeled ammonia concentrations were much lower than the retrieved ammonia concentrations at the aircraft height. This was also found when comparing the modeled total column loading of ammonia with the total column loading of ammonia retrieved by TES.

Table 2. Comparison of CMAQ model predictions at the aircraft level and the total column loading with the corresponding TES retrievals for NH_3.

	NH_3 At aircraft level ($\mu g\ m^{-3}$)	NH_3 Total column loading ($mg\ m^{-2}$)
TES retrievals		
Average	14.8	7.2
Standard deviation	11.8	6.7
Maximum	40.5	40.4
Median	10.4	5.1
Model predictions		
Average	3.3	0.002
Standard deviation	1.0	0.002
Maximum	4.9	0.008
Median	3.4	0.002
Comparison statistics		
Normalized mean bias of TES retrieval	-77%	-99%
Ratio of average TES retrieval value to average modeled	4.5	3600
Ratio of median measured value to median modeled value	3.1	2550
Correlation coefficient (r)	0.28	0.54
Coefficient of determination (r^2)	0.08	0.30
Number of observations	12	66

3.3. Satellite Retrievals Compared with In-Situ Aircraft Measurements

In this study, only 12 satellite retrievals with adequate data quality lined up with the aircraft measurements taken during the CalNex study (Figure 8), therefore limiting the results. Table 3 and Figure 9 compare the *in-situ* aircraft measurements with the satellite observations obtained from TES. The average corresponding NH_3 concentration measured from the CalNex campaign was found to be $33.1 \pm 35.5\ \mu g\ m^{-3}$, with a maximum NH_3 concentration of $108.8\ \mu g\ m^{-3}$ and a median value of $10.2\ \mu g\ m^{-3}$. In comparison to this, the average TES NH_3 concentration was $14.8 \pm 11.8\ \mu g\ m^{-3}$, with a maximum measured concentration of $40.5\ \mu g\ m^{-3}$. However, the median value observed for the TES NH_3 concentration was $10.4\ \mu g\ m^{-}3$, which is similar to that of the NH_3 aircraft measurements median. Thus, the ratio of the median measured value to the median modeled value is 0.98.

Figure 8. The 12 locations where the CalNex *in-situ* measurements could be compared with the TES satellite retrieval of NH_3. The pink colored triangles represent the locations where the *in-situ* and satellite measurements were compared while the blue polygons represent the major cities in California.

As Figure 9 shows, the majority of the NH_3 measurements fall above the one to one line. This normalized mean bias of the TES retrieval was found to be -55%, which corresponds to a ratio of the average measured NH_3 value to the average NH_3 TES retrieval of 2.2. The median of the in-situ aircraft measurements was 10.2 $\mu g\ m^{-3}$, while the median of the CMAQ measurements was 10.4 $\mu g\ m^{-3}$, which corresponds with a median ratio of 0.98. As mentioned in the previous section, a source of error when comparing the TES retrieval with the CMAQ data is the fact that the two data sources were not entirely aligned in both space and time.

Table 3. Comparison of *in-situ* aircraft measurements with TES retrievals for NH_3.

	NH_3 ($\mu g\ m^{-3}$)
***In situ* aircraft measurements**	
Average	33.1
Standard deviation	35.5
Maximum	108.8
Median	10.2
TES retrievals	
Average	14.8
Standard deviation	11.8
Maximum	40.5
Median	10.4
Comparison statistics	
Normalized mean bias of TES retrieval	-55%
Ratio of average measured value to average TES retrieval	2.2
Ratio of median measured value to median modeled value	0.98
Correlation coefficient (r)	0.25
Coefficient of determination (r^2)	0.06
Number of observations	12

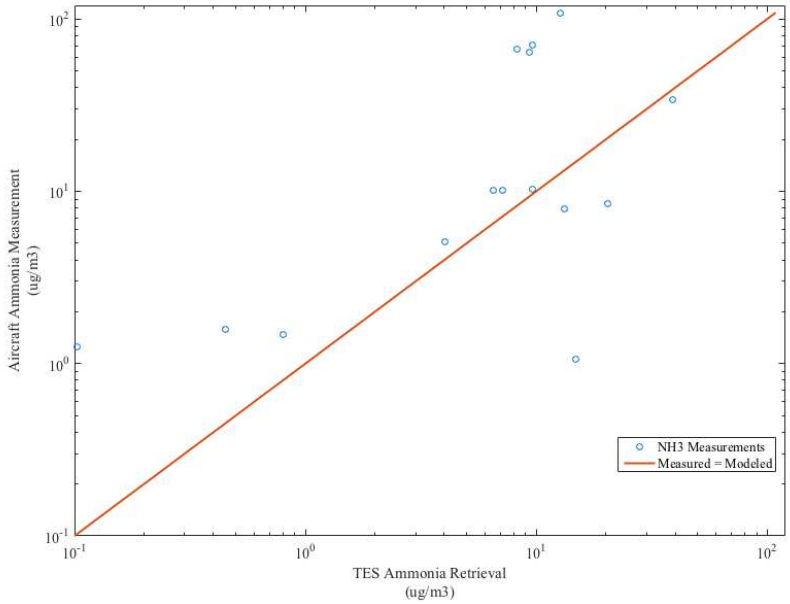

Figure 9. Compares the *in-situ* aircraft measurements with the satellite observations obtained from TES on a log-log scale plot. The solid red line shows where the measured points should have fallen if the model predictions were exactly correct. The TES NH_3 retrievals were much closer to the observed aircraft measurements when compared with the model output.

3.4. Analysis of Model Bias in Relation to Previous Studies and the NH_3 Emissions Inventory

Several studies have been conducted to determine how well the CMAQ model can predict NH_3 concentration. In general, it has been found that the CMAQ model has a tendency to under predict NH_3 concentrations, particularly over large source regions (Table 4) (Gilliland *et al.*, 2006; Kelly *et al.*, 2014; Butler *et al.,* 2015; Schifer *et al.,* 2016; Battye *et al.*, 2016). Gilliland *et al.* (2006) used an inverse modeling technique with CMAQ v4.4 to predict NH3 emissions for the continental United States (CONUS). The results of this study indicated that the emissions inventory is too high for the winter months and too low for the summer months. Similar results were found by Butler *et al.* (2015), who used CMAQ v4.7.1 to predict NH3 concentrations in Susquehanna River Watershed of New York and Pennsylvania. When comparing ambient concentration measurements of NH_3 with the model predictions, it was found that the model under estimated concentration by 8-60%. In addition to this, it was also found that the NH_3 under estimations were particularly high over the agricultural regions. Kelly *et al.* (2014) found similar results when comparing NH_3 measurements obtained from the California Research at the Nexus of Air Quality and Climate Change (CalNex) field campaign that occurred May-June, 2010, with model predictions from CMAQ v5.0.2. In addition to this, it was also found that the CMAQ model also predicted lower concentrations of NH_3 in some urban regions as well. Battye *et al.* (2016) found comparable results to Kelly *et al.* (2014) when comparing NH_3 measurements from the Deriving Information on Surface conditions from Column and Vertically Resolved Observations Relevant to Air Quality (DISCOVER AQ) field campaign (July-August, 2014) with NOAA's NAQFC CMAQ model (v5.0.2) over the agricultural regions of northeastern Colorado. Schifer *et al.* (2016) used GEOS-Chem (v9-02, driven by GEOS-5 assimilated meteorology) to simulate concentrations of atmospheric ammonia across the United States from 2008 to 2012 and found that the model tended to under predict ammonia concentrations near large source regions, under predicting concentrations by 26% when compared with surface sites. The current study found similar results to Gilliland *et al.* (2006), Kelly *et al.* (2014), Butler *et al.* (2015), Schifer *et al.* (2016) and Battye *et al.* (2016), where the CMAQ model (v4.6) under estimates NH_3 concentration, with the results being most comparable to Kelly *et al.* (2014) and Battye *et al.* (2016).

Meteorological factors can have a major impact on the emission and removal processes of ammonia. Both wind speed and relative humidity have been found to be inversely proportional to ammonia concentrations (Flechard and Fowler, 1998; Kapoor *et al.,* 1992; Parmar *et al*., 2001; Phillips *et al*., 2004; Sharma *et al.,* 2010; Sharma *et al.,* 2011), while temperature was primarily found to be directly proportional to ammonia concentrations (Flechard and Fowler, 1998). Ammonia concentrations tend to be lower during clear skies and when precipitation occurred (Kapoor *et al.,* 1992). Schifer *et al.* (2016) also notes the importance of meteorology in atmospheric air quality. They found that meteorology contributed to 64% of the changes in the surface concentration of ammonia when compared with reductions air pollution. Therefore, errors in the meteorology used within the CMAQ model could have contributed to the large under estimations observed in this study.

Another potential source of error in NH_3 predictions is the absence of the bidirectional flux model within the CMAQ version used. Cooter *et al.* (2012) and Bash *et al.* (2013) found that the use of the bidirectional flux in the model increases NH_3 concentrations on average by about 10% over the continental US. It is important to note that the flux will likely be higher over agricultural regions due to the abundance of NH_3 in the agricultural

cropping system. Error in the model processes used to handle NH_3 emissions may also contribute to the observed bias. For example, the 12 km spatial resolution may lead to the model overlooking high concentrations that are smaller than the grid size. However, the similar results found by Kelly *et al.* (2014), who used an updated version (5.0.1) of the CMAQ model with a 4km vertical resolution and 34 vertical layers, suggest that this is not entirely the cause of the under estimation. Another likely source of error is the use of older National Emissions Inventories (NEI). For example, Gilliland *et al.* (2006) used the 2001 NEI while Battye *et al.* (2016) and this current study used the 2005 NEI. Recall from the above discussion that the NH_3 emissions increased 25% between the 2005 and 2011 (EPA, 2005; EPA, 2011). In contrast to this, NH_3 emissions increased 85% from the 2005 NEI to the 2014 NEI after major changes were made to the methodologies used to calculate the agricultural emissions of ammonia. In addition, it is possible that an increase in animal activity could have contributed to the increase in NH_3 emission. Because the majority of the under estimations, both in this study and the literature, tend to occur over agricultural regions, it is likely that a major contributor to this under estimation of NH_3 concentrations is due to an under estimation of NH_3 emissions from agricultural sources in the US National Emissions Inventories used in most research (i.e. inventories that are older than the current 2014 NEI).

4. Conclusion

The NOAA NAQFC CMAQ model under predicted NH_3 concentrations in California measured during the CalNex2010 field campaign by a factor of 2.4 (NMB = -58%), with a median ratio of 0.8. Similarly, the NOAA NAQFC CMAQ model under predicted NH_3 concentrations in California by a factor of 4.5 (NMB = -77%), with a median ratio of 3.1, when compared with measurements obtained from TES. In contrast to this, the CMAQ model had a fairly good handle on NH4+ concentrations, only over predicting by a factor of 0.7 (NMB = 43%), with a median ratio of 0.7. When comparing the median values for NH_3 and NH_4^+, it was found that the median values were fairly similar for both modeled and measured values. Despite the model under estimating NH_3 concentrations, particularly at high concentrations the NH_4^+ projections were fairly accurate, which suggests that the issue lies within the prediction of gaseous NH_3. These results indicate that while the NOAA CMAQ model represents the partitioning of NH_3, there is still uncertainty in predicting concentrations of gaseous NH_3. This also suggests that the NH_3 levels in California exceed the levels of the acidic species necessary for the gas-to-particle conversion. Therefore, this will have major implications for $PM_{2.5}$ reduction strategies. In addition to this, it is important to note that a portion of the error in comparing the TES retrieval measurements with the CMAQ model prediction is likely due to the fact that the retrieval and the predicted concentration did not line up completely in space and time.

Recall that there are at least four potential sources of error within the CMAQ model: the lack of the inclusion of the bidirectional flux model, potential errors in the model processes used, errors within the NH_3 emissions used in the model and errors in the meteorology used within the models. The addition of bidirectional flux to the model would increase NH_3 emissions, particularly over the agricultural regions, and therefore likely contributes to the model bias observed in this study. Similarly, ammonia emissions in the 2014 NEI increased

85% from the emissions calculated by the 2005 NEI, primarily due to the update in the methodologies used to calculate agricultural emissions of ammonia. Because the majority of the highest model bias occur in areas of agriculture, it is likely that a major part of the problem lies within the agricultural emissions of NH_3 in the 2005 NEI. Other potential sources of the observed bias include the changes made to the diurnal and temporal representation of ammonia emissions within the NEI as well as errors with the meteorology used within the models. Based on the results of this study, it seems that the two major sources of error within the model lies with the 2005 NEI NH_3 emissions and the lack of the bidirectional flux model used in the model.

Acknowledgements

We acknowledge the generous help and guidance of Dr. Andy Neuman (NOAA), Dr. Ann Middlebrook (NOAA) and Dr. Roya Bahreini (UCR), the NCSU Air Quality Research Group, the NOAA National Air Quality Forecast Program, and the CalNex2010 field campaign. The ammonia satellite data was retrieved from NASA TES instrument on the Aura satellite. We would also like to acknowledge the Kenan fund.

References

Anderson, N., Strader, R., Davidson, C., 2003. Airborne reduced nitrogen: ammonia emissions from agriculture and other sources. Environment International 29, 277–286. doi:10.1016/s0160-4120(02)00186-1

Aneja, V.P., Schlesinger, W.H., Erisman, J.W., 2009. Effects of Agriculture upon the Air Quality and Climate: Research, Policy, and Regulations. Environmental Science & Technology Environ. Sci. Technol. 43, 4234–4240. doi:10.1021/es8024403

(a) Baek, B.H., Aneja, V.P., Tong, Q., 2004. Chemical coupling between ammonia, acid gases, and fine particles. Environmental Pollution 129, 89–98. doi:10.1016/j.envpol.2003.09.022

(b) Baek, B.H., Aneja, V.P., 2004. Measurement and Analysis of the Relationship between Ammonia, Acid Gases, and Fine Particles in Eastern North Carolina. Journal of the Air & Waste Management Association 54, 623–633. doi:10.1080/10473289.2004.10470933

Bahreini, R., Ervens, B., Middlebrook, A.M., Warneke, C., Gouw, J.A.D., Decarlo, P.F., Jimenez, J.L., Brock, C.A., Neuman, J.A., Ryerson, T.B., Stark, H., Atlas, E., Brioude, J., Fried, A., Holloway, J.S., Peischl, J., Richter, D., Walega, J., Weibring, P., Wollny, A.G., Fehsenfeld, F.C., 2009. Organic aerosol formation in urban and industrial plumes near Houston and Dallas, Texas. J. Geophys. Res. Journal of Geophysical Research 114. doi:10.1029/2008jd011493

Bahreini, R., Middlebrook, A.M., Gouw, J.A.D., Warneke, C., Trainer, M., Brock, C.A., Stark, H., Brown, S.S., Dube, W.P., Gilman, J.B., Hall, K., Holloway, J.S., Kuster, W.C., Perring, A.E., Prevot, A.S.H., Schwarz, J.P., Spackman, J.R., Szidat, S., Wagner, N.L., Weber, R.J., Zotter, P., Parrish, D.D., 2012. Gasoline emissions dominate over diesel in formation of secondary organic aerosol mass. Geophys. Res. Lett. Geophysical Research Letters 39. doi:10.1029/2011gl050718

Bash, J.O., Cooter, E.J., Dennis, R.L., Walker, J.T., Pleim, J.E., 2013. Evaluation of a regional air-quality model with bidirectional NH3 exchange coupled to an agroecosystem model. Biogeosciences 10, 1635–1645. doi:10.5194/bg-10-1635-2013

Battye, W.H., Bray, C.D., Aneja, V.P., Tong, D., Lee, P., Tang, Y., 2016. Evaluating ammonia (NH3) predictions in the NOAA National Air Quality Forecast Capability (NAQFC) using in situ aircraft, ground-level, and satellite measurements from the DISCOVER-AQ Colorado campaign. Atmospheric Environment 140, 342–351. doi:10.1016/j.atmosenv.2016.06.021

Beer, R., Glavich, T.A., Rider, D.M., 2001. Tropospheric emission spectrometer for the earth observing System's aura satellite. Applied Optics 40, 2356-2367.

Beer, R., 2006. TES on the aura mission: Scientific objectives, measurements, and analysis overview. IEEE Transactions on Geoscience and Remote Sensing 44, 1102-1105.

(a) Behera, S.N., Sharma, M., 2010. Investigating the potential role of ammonia in ion chemistry of fine particulate matter formation for an urban environment. Science of The Total Environment 408, 3569–3575. doi:10.1016/j.scitotenv.2010.04.017

(b) Behera, S.N., Sharma, M., 2010. Investigating the potential role of ammonia in ion chemistry of fine particulate matter formation for an urban environment. Science of The Total Environment 408, 3569–3575. doi:10.1016/j.scitotenv.2010.04.017

Bowman, K.W., Rodgers, C.D., Kulawik, S.S., Worden, J., Sarkissian, E., Osterman, G., Steck, T., Lou, M., Eldering, A., Shephard, M., 2006. Tropospheric emission spectrometer: Retrieval method and error analysis. IEEE Transactions on Geoscience and Remote Sensing 44, 1297-1307.

Butler, T., Marino, R., Schwede, D., Howarth, R., Sparks, J., Sparks, K., 2014. Atmospheric ammonia measurements at low concentration sites in the northeastern USA: implications for total nitrogen deposition and comparison with CMAQ estimates. Biogeochemistry 122, 191–210. doi:10.1007/s10533-014-0036-5

Canty, T. P., Hembeck, L., Vinciguerra, T. P., Anderson, D. C., Goldberg, D. L., Carpenter, S. F., Allen, D. J., Loughner, C. P., Salawitch, R. J., Dickerson, R. R., 2015. Ozone and NOx chemistry in the eastern US: evaluation of CMAQ/CB05 with satellite (OMI) data. Atmos. Chem. Phys., 15, 10965-10982, doi:10.5194/acp-15-10965-2015, 2015.

Clarisse, L., Shephard, M.W., Dentener, F., Hurtmans, D., Cady-Pereira, K., Karagulian, F., Van Damme, M., Clerbaux, C., Coheur, P., 2010. Satellite monitoring of ammonia: A case study of the San Joaquin Valley. Journal of Geophysical Research: Atmospheres 115.

Cooter, E.J., Bash, J.O., Benson, V., Ran, L., 2012. Linking agricultural crop management and air quality models for regional to national-scale nitrogen assessments. Biogeosciences 9, 4023–4035. doi:10.5194/bg-9-4023-2012

Duncan, B.N., Lamsal, L.N., Thompson, A.M., Yoshida, Y., Lu, Z., Streets, D.G., Hurwitz, M.M., Pickering, K.E., 2016. A space-based, high-resolution view of notable changes in urban NOx pollution around the world (2005–2014). Journal of Geophysical Research: Atmospheres 121, doi:10.1002/2015JD024121.

EPA, 2005. 2005 National Emissions Inventory. Accessed March 2017. ftp://ftp.epa.gov/EmisInventory/2005_nei/.

EPA, 2011. 2011 National Emissions Inventory. Accessed March 2017. ftp://ftp.epa.gov/EmisInventory/2011nei/.

EPA, 2014. 2014 National Emissions Inventory. Accessed March 2017. ftp://ftp.epa.gov/EmisInventory/2014/.

EPA, 2016. 2014 National Emissions Inventory Technical Supporting Document. Accessed March 2017. https://www.epa.gov/sites/production/files/2016-12/documents/nei2014v1_tsd.pdf.

Fan, J., Zhang, R., Li, G., Nielsen-Gammon, J. Li, Z., 2005. Simulations of fine particulate matter (PM2. 5) in Houston, Texas. Journal of Geophysical Research: Atmospheres, 110(D16).

Flechard, C. R., Fowler, D. (1998). Atmospheric ammonia at a moorland site. I: The meteorological control of ambient ammonia concentrations and the influence of local sources. Q.J Royal Met. Soc. Quarterly Journal of the Royal Meteorological Society, 124, 733–757. doi:10.1002/qj.49712454705

Gilliland, A.B., Appel, K.W., Pinder, R.W., Dennis, R.L., 2006. Seasonal NH3 emissions for the continental united states: Inverse model estimation and evaluation. Atmospheric Environment 40, 4986–4998. doi:10.1016/j.atmosenv.2005.12.066

Heald, C.L., Jr., J.L.C., Lee, T., Benedict, K.B., Schwandner, F.M., Li, Y., Clarisse, L., Hurtmans, D.R., Damme, M.V., Clerbaux, C., Coheur, P.-F., Philip, S., Martin, R.V., Pye, H.O.T., 2012. Atmospheric ammonia and particulate inorganic nitrogen over the United States. Atmospheric Chemistry and Physics Atmos. Chem. Phys. 12, 10295–10312. doi:10.5194/acp-12-10295-2012

Herman R, Osterman G., 2014. Earth Observing System (EOS) Tropospheric Emission Spectrometer (TES): Data Validation Report. Accessed March 2017. https://eosweb.larc.nasa.gov/sites/default/files/project/tes/readme/TES_Validation_Report_v6.pdf

Kapoor, R., Singh, G.,Tiwari, S., 1992. Ammonia concentration vis-a-vis meteorological conditions at Delhi, India. Atmospheric Research, 28, 1–9.

Kelly, J.T., Baker, K.R., Nowak, J.B., Murphy, J.G., Markovic, M.Z., Vandenboer, T.C., Ellis, R.A., Neuman, J.A., Weber, R.J., Roberts, J.M., Veres, P.R., Gouw, J.A.D., Beaver, M.R., Newman, S., Misenis, C., 2014. Fine-scale simulation of ammonium and nitrate over the South Coast Air Basin and San Joaquin Valley of California during CalNex-2010. Journal of Geophysical Research: Atmospheres J. Geophys. Res. Atmos. 119, 3600–3614. doi:10.1002/2013jd021290

Kwok, R., Napelenok, S., Baker, K., 2013. Implementation and evaluation of PM2.5 source contribution analysis in a photochemical model. Atmospheric Environment 80, 398–407. doi:10.1016/j.atmosenv.2013.08.017

Nowak, J.B., Neuman, J.A., Bahreini, R., Brock, C.A., Middlebrook, A.M., Wollny, A.G., Holloway, J.S., Peischl, J., Ryerson, T.B., Fehsenfeld, F.C., 2010. Airborne observations of ammonia and ammonium nitrate formation over Houston, Texas. J. Geophys. Res. Journal of Geophysical Research 115. doi:10.1029/2010jd014195

Nowak, J.B., Neuman, J.A., Bahreini, R., Middlebrook, A.M., Holloway, J.S., Mckeen, S.A., Parrish, D.D., Ryerson, T.B., Trainer, M., 2012. Ammonia sources in the California South Coast Air Basin and their impact on ammonium nitrate formation. Geophys. Res. Lett. Geophysical Research Letters 39. doi:10.1029/2012gl051197

Pan, L., Tong, D., Lee, P., Kim, H.C. Chai, T., 2014. Assessment of NO x and O 3 forecasting performances in the US National Air Quality Forecasting Capability before and after the 2012 major emissions updates. Atmospheric Environment, 95, pp.610-619.

Parmar R.S., Satsangi, G.S., Lakhani. A., 2001. Simultaneous measurements of ammonia and nitric acid in ambient air at Agra (27o10′N and 78o05′E) (India). Atmospheric Environment, 35, 5979-5988.

Phillips, S. B., Arya, S. P., Aneja, V. P., 2004. Ammonia flux and dry deposition velocity from near-surface concentration gradient measurements over a grass surface in North Carolina. Atmospheric Environment, 38, 3469–3480. doi:10.1016/j.atmosenv.2004.02.054

Pope, C.A., Ezzati, M., Dockery, D.W., 2009. Fine-Particulate Air Pollution and Life Expectancy in the United States. New England Journal of Medicine N Engl J Med 360, 376–386. doi:10.1056/nejmsa0805646

Renner, E., Wolke, R., 2010. Modelling the formation and atmospheric transport of secondary inorganic aerosols with special attention to regions with high ammonia emissions. Atmospheric Environment 44, 1904–1912. doi:10.1016/j.atmosenv.2010.02.018

Robarge, W.P., Walker, J.T., Mcculloch, R.B., Murray, G., 2002. Atmospheric concentrations of ammonia and ammonium at an agricultural site in the southeast United States. Atmospheric Environment 36, 1661–1674. doi:10.1016/s1352-2310(02)00171-1

Ryerson, T.B., Andrews, A.E., Angevine, W.M., Bates, T.S., Brock, C.A., Cairns, B., Cohen, R.C., Cooper, O.R., Gouw, J.A.D., Fehsenfeld, F.C., Ferrare, R.A., Fischer, M.L., Flagan, R.C., Goldstein, A.H., Hair, J.W., Hardesty, R.M., Hostetler, C.A., Jimenez, J.L., Langford, A.O., Mccauley, E., Mckeen, S.A., Molina, L.T., Nenes, A., Oltmans, S.J., Parrish, D.D., Pederson, J.R., Pierce, R.B., Prather, K., Quinn, P.K., Seinfeld, J.H., Senff, C.J., Sorooshian, A., Stutz, J., Surratt, J.D., Trainer, M., Volkamer, R., Williams, E.J., Wofsy, S.C., 2013. The 2010 California Research at the Nexus of Air Quality and Climate Change (CalNex) field study. Journal of Geophysical Research: Atmospheres J. Geophys. Res. Atmos. 118, 5830–5866. doi:10.1002/jgrd.50331

Schiferl, L.D., Heald, C.L., Van Damme, M., Clarisse, L., Clerbaux, C., Coheur, P.F., Nowak, J.B., Neuman, J.A., Herndon, S.C., Roscioli, J.R. Eilerman, S.J., 2016. Interannual variability of ammonia concentrations over the United States: sources and implications. Atmospheric Chemistry and Physics, 16(18), pp.12305-12328.

Sharma, S.K., Datta, A., Saud, T., 2010. Seasonal variability of ambient NH3, NO, NO2 and SO2 over Delhi. Journal of Environmental Sciences, 22, 1023-1028

Sharma, S. K., Pathak, H., Datta, A., Saxena, M., Saud, T., Mandal, T. K., 2011. Study on mixing ratio of atmospheric ammonia and other nitrogen components. Proceedings of the International Academy of Ecology and Environmental Sciences, 1.

Shephard, M., Cady-Pereira, K., 2015. Cross-track infrared sounder (CrIS) satellite observations of tropospheric ammonia. Atmospheric Measurement Techniques 8, 1323-1336.

Shephard, M., Cady-Pereira, K., Luo, M., Henze, D., Pinder, R., Walker, J., Rinsland, C., Bash, J., Zhu, L., Payne, V., 2011. TES ammonia retrieval strategy and global observations of the spatial and seasonal variability of ammonia. Atmospheric chemistry and physics 11, 10743-10763.

Tong, D.Q., Lamsal, L., Pan, L., Ding, C., Kim, H., Lee, P., Chai, T., Pickering, K.E., Stajner, I., 2015. Long-term NO x trends over large cities in the United States during the great recession: Comparison of satellite retrievals, ground observations, and emission inventories. Atmospheric Environment, 107, pp.70-84.

Wang, X., Wang, W., Yang, L., Gao, X., Nie, W., Yu, Y., Xu, P., Zhou, Y., Wang, Z., 2012. The secondary formation of inorganic aerosols in the droplet mode through heterogeneous aqueous reactions under haze conditions. Atmospheric Environment 63, 68–76. doi:10.1016/j.atmosenv.2012.09.029

Zhu, L., Henze, D., Cady-Pereira, K., Shephard, M., Luo, M., Pinder, R., Bash, J., Jeong, G., 2013. Constraining US ammonia emissions using TES remote sensing observations and the GEOS-Chem adjoint model. Journal of Geophysical Research: Atmospheres 118, 3355-3368.

Zhu, L., Henze, D.K., Bash, J.O., Jeong, G-R., Cady-Pereira, K.E., Shephard, M.W., Luo, M., Poulot, F., Capps, S., 2015, Global evaluation of ammonia bi-directional exchange and livestock diurnal variation schemes, Atmos. Chem. Phys., 15, 12823-12843, doi:10.5194/acp-15-12823-2015